

ORIGINAL ARTICLE

The influence of genetic variants on striatal dopamine transporter and D2 receptor binding after TBI

Amy K Wagner^{1,2}, Joelle M Scanlon¹, Carl R Becker³, Anne C Ritter¹, Christian Niyonkuru¹, Clifton E Dixon^{1,2,4}, Yvette P Conley^{2,5} and Julie C Price³

Dopamine (DA) neurotransmission influences cognition and recovery after traumatic brain injury (TBI). We explored whether functional genetic variants affecting the DA transporter (DAT) and D2 receptor (DRD2) impacted *in vivo* dopaminergic binding with positron emission tomography (PET) using [¹¹C]β-CFT and [¹¹C]raclopride. We examined subjects with moderate/severe TBI (*N* = 12) ~ 1 year post injury and similarly matched healthy controls (*N* = 13). The variable number of tandem repeat polymorphism within the DAT gene and the TaqI restriction fragment length polymorphism near the DRD2 gene were assessed. TBI subjects had age-adjusted DAT-binding reductions in the caudate, putamen, and ventral striatum, and modestly increased D2 binding in ventral striatum versus controls. Despite small sample sizes, multivariate analysis showed lower caudate and putamen DAT binding among DAT 9-allele carriers and DRD2 A2/A2 homozygotes with TBI versus controls with the same genotype. Among TBI subjects, 9-allele carriers had lower caudate and putamen binding than 10/10 homozygotes. This PET study suggests a hypodopaminergic environment and altered DRD2 autoreceptor DAT interactions that may influence DA transmission after TBI. Future work will relate these findings to cognitive performance; future studies are required to determine how DRD2/DAT1 genotype and DA-ligand binding are associated with neurostimulant response and TBI recovery.

Journal of Cerebral Blood Flow & Metabolism (2014) **34**, 1328–1339; doi:10.1038/jcbfm.2014.87; published online 21 May 2014

Keywords: β-CFT; dopamine; genetic variation; PET imaging; raclopride; traumatic brain injury

INTRODUCTION

Dopamine (DA) neurons originate in the substantia nigra and project to cerebral forebrain structures, including hippocampus, prefrontal cortex, and striatum. The striatum is a part of an anatomic network that subserves functions associated with the dorsolateral prefrontal cortex. Further, the striatum helps mediate cognition in humans.¹ Also, accumulating evidence supports a 'dopaminergic hypothesis' as important to traumatic brain injury (TBI) recovery.² Evidence supporting this hypothesis includes our previous work showing elevated dopamine (DA) levels in cerebrospinal fluid (CSF) in response to ICU treatments and innate factors like sex and DA transporter (DAT) genetic variation.³ Previous studies show striatal DAT binding reductions after severe TBI,⁴ which are supported by experimental TBI studies using real time neurotransmission approaches demonstrating reduced maximal evoked DA overflow and altered DA clearance kinetics in striatum.⁵ DAT protein expression changes also have been documented with experimental TBI.^{5,6}

Previous work supports TBI practice guidelines for using the DAT inhibitor, methylphenidate (MPD), to improve cognition.⁷ Multiple DA agonists, including MPD, have beneficial effects on spatial learning in experimental TBI, although sex differences in MPD induced behavioral changes and cognitive benefit have been noted after controlled cortical impact (CCI) injury.² The neurobiology of striatal DA transmission deficits is not fully

characterized in experimental TBI. However, daily MPD has restorative effects on striatal neurotransmission after CCI.⁶ Despite its effectiveness, not all patients improve with MPD treatment. Further, clinical studies stratifying sex, age, and genetic makeup have not been conducted, making personalized use challenging with optimizing drug efficacy in treating cognitive deficits associated with TBI.

Several DA genetic variants are associated with multiple neurologic, cognitive, and psychiatric conditions,^{8–11} and many associated symptoms overlap with deficits observed with TBI. Given the influence of DA systems on TBI pathology and recovery, along with how DA variants contribute to neurologic diseases with symptom profiles similar to TBI symptomatology, we hypothesized that moderate-to-severe TBI would alter striatal DAT/D2R binding chronically relative to control subjects. Thus, we explored the most appropriate methods from which to assess striatal DA systems in a TBI population and whether genetic variability influences striatal DAT and D2 receptor (D2R) binding using positron emission tomography (PET) with [¹¹C]β-CFT and [¹¹C]raclopride.

MATERIALS AND METHODS

Participants

In accordance with the ethical principles stated in the Belmont Report (<http://www.hhs.gov/ohrp/humansubjects/guidance/belmont.html>) and other regulations for protection of human subjects outlined by the United States

¹Department of Physical Medicine and Rehabilitation, School of Medicine, University of Pittsburgh, Pittsburgh, Pennsylvania, USA; ²Safar Center for Resuscitation Research, University of Pittsburgh, Pittsburgh, Pennsylvania, USA; ³Department of Radiology, School of Medicine, University of Pittsburgh, Pittsburgh, Pennsylvania, USA; ⁴Department of Neurosurgery, School of Medicine, University of Pittsburgh, Pittsburgh, Pennsylvania, USA and ⁵Department of Health Promotion & Development, School of Nursing, University of Pittsburgh, Pittsburgh, Pennsylvania. Correspondence: Dr AK Wagner, Department of Physical Medicine and Rehabilitation, University of Pittsburgh, 3471 Fifth Avenue, Suite 202, Pittsburgh, PA 15213, USA. or Professor JC Price, Department of Radiology, School of Medicine, University of Pittsburgh, PET Facility, PUH B-938, 200 Lothrop Street, Pittsburgh, PA 15213, USA.

E-mail: wagnerak@upmc.edu or pricjc@upmc.edu

Support for this work was provided by NIH R01 HD048162; K01 MH01976.

Received 3 January 2014; revised 12 March 2014; accepted 21 April 2014; published online 21 May 2014

Health and Human Services (<http://www.hhs.gov/ohrp/humansubjects/guidance/45cfr46.html>), this study was approved by the University of Pittsburgh Institutional Review Board. Twelve adult Caucasian men with moderate/severe TBI (admission Glasgow Coma Score (GCS) 3 to 12 obtained within 6 hours post injury) and executive function deficits, based on neuropsychological testing 1 year post injury, were recruited. Potential subjects with TBI were excluded for penetrating head injuries, significant neurologic condition (other than TBI), history of significant drug or alcohol abuse in the past year, magnetic resonance imaging (MRI) contraindication, certain neuroactive medications, or medications known to interact with dopaminergic systems. Data on alcohol, caffeine, tobacco, and medication use was obtained by participant self-report at the time of imaging. Thirteen healthy controls were enrolled on the basis of similar factors. Data characterizing recruited TBI subjects included DAT1/DRD2 genotype, age, race, sex, educational status, mechanism, and type of injury. TBI subjects were included if they had diffuse axonal injury, intraparenchymal frontal lobe pathology (including significant midline shift), or injury involving the striatum. DAT1/DRD2 genotype, age, and educational status were collected for healthy controls to match enrolled TBI subjects.

Genotyping DRD2 and DAT1

DRD2 gene: TaqI RFLP. Amplified DNA underwent 30 cycles of denaturation at 95 °C for 1 minute, annealing at 58 °C for 30 seconds, and extension at 72 °C for 1 minute, to amplify the 459 bp product, which was then exposed to TaqIA restriction endonuclease to perform the restriction fragment length polymorphism analysis. Digested products were electrophoresed on a 3% agarose gel, stained with ethidium bromide for DNA band detection, and assigned a genotype based on presence/absence of original or cut DNA fragments. Primers used were 5'-CCGTCGACCTTCTCTAGTGCATCA-3' and 5'-CCGTCGACGGCTGGCCAAGTTGTCTA-3'.

DAT1 gene (SLC6A3) 3' UTR VNTR. Amplified DNA underwent 30 cycles of denaturation at 95 °C for 1 minute, annealing at 62 °C for 30 seconds, and extension at 72 °C for 1 minute, to amplify the 280–600 bp product, which was then electrophoresed on a 1% agarose/2% nusieve gel, stained with ethidium bromide for DNA band detection, and assigned a genotype based on allele sizes. Primers used were 5'-TGTGGTGTAGGGAACGGCCTGAG-3' and 5'-CTTCTGGAGTACGGCTCAAGC-3'.

Magnetic Resonance Imaging

T1-weighted structural three-dimensional MRI data were acquired using sequences optimized for gray matter, white matter and cerebrospinal fluid (CSF) contrast. Magnetic resonance imaging was performed using a 1.5 Tesla GE Signa scanner, parameters described by Drevets¹² and a 3 Tesla Siemens Magnetom Trio scanner (TR/TE = 5/25 ms; flip angle = 40°; field of view = 24 × 18 cm, slice thickness = 1.5 mm, in-plane resolution 0.94 × 0.94 mm).

Positron Emission Tomography Imaging and Blood Sampling

Dopamine transporter imaging was performed using [¹¹C]β-CFT, a DA reuptake inhibitor with moderate affinity, relatively slow *in vivo* kinetics, and good selectivity for DAT over serotonin transporters.¹³ Rodent studies support CFT ligand selectivity, with one report showing CFT ([¹⁸F]CFT) did not bind to rat SERT.¹⁴ Also, although ([³H]CFT) was found to have human NET binding properties,¹⁵ previous work suggests that DAT is the primary transporter located in striatum,¹⁶ thus minimizing the impact of NET on DA clearance and the specificity of CFT for DAT binding in our striatal regions of interest.

Dopamine D2 receptor (D2R) imaging was performed using [¹¹C]raclopride ([¹¹C]RAC), a D2/D3 receptor antagonist with relatively higher affinity and reversible *in vivo* kinetics. The binding affinity for D2R receptors is similar to D3R receptors.¹⁷ Thus it is not possible to differentiate binding for these two receptors within our PET design. However, [¹¹C]RAC binds primarily to D2R in dorsal putamen and caudate because of minimal D3 receptor expression in these regions, and it exhibits mixed binding (2/3-D2R; 1/3-D3R) in ventral striatum.¹⁸

Both radiotracers were produced using remotely controlled radio-syntheses.^{19,20} Chemical and radiochemical purities reached ≥95%, with specific activities ≥2000 Ci/mmol at the end of synthesis. Positron emission tomography scans were acquired on a Siemens/CTI ECAT HR + scanner (3D-mode, 63-planes, 15.2 cm axial field of view) equipped with a Neuro-insert to reduce scattered photon events. Before PET imaging, an intravenous catheter was placed in an antecubital vein for radiotracer

injection, and a short catheter was inserted into a radial artery for dynamic arterial blood sampling. Head motion was minimized using thermoplastic mask immobilization. Subjects were positioned in the scanner with imaging planes parallel to the canthomeatal line, and primary areas of interest (including cerebellum) within the central 7 cm of the field of view. A windowed transmission scan (⁶⁸Ge/⁶⁸Ga) was performed for attenuation correction. Positron emission tomography emission data were corrected for dead-time, radioactive decay and scatter, with filtered-back projection image reconstruction (final resolution ~6 mm). Dynamic PET scanning and manual arterial blood sampling were performed over either 90 minutes ([¹¹C]β-CFT: 35 time frames; 35 blood samples) or 60 minutes ([¹¹C]RAC: 22 time frames; 33 blood samples), with five additional samples used to determine the concentration of radiolabeled metabolites of [¹¹C]β-CFT²¹ or [¹¹C]RAC,¹² relative to total plasma radioactivity. A multi-exponential curve was fit to the fractional values of unmetabolized radiotracer in plasma over time and used to generate a metabolite-corrected arterial input function for each radiotracer.

Image Processing and Analyses

The MRI data were co-registered to the [¹¹C]β-CFT and [¹¹C]RAC PET data using automated image registration methods previously described.¹² Magnetic resonance and PET images were re-sliced to be parallel to the intercommissural anterior commissure–posterior commissure line in the axial plane for consistent region-of-interest (ROI) delineation and sampling across subjects. Regions of interest were defined across several MRI planes using a modified version of ROITool (CTI PET Systems). Regions of interest included caudate (seven planes: four superior, three middle), ventral striatum (three planes: encompassing accumbens shell), putamen (three planes), and cerebellum.¹² Additional caudate and putamen regions were drawn dorsally. The cerebellar ROI sampled the superior portion of the posterior lobule avoiding vermis and white matter. Right and left hemisphere ROIs were grouped, as laterality differences in binding were not hypothesized. Regions of interest were applied to co-registered dynamic PET data to generate regional time-activity curves (Figure 1). Due to chronic morphological changes resulting from TBI, MRI data were used to assess cerebral atrophy as represented by dilutional effects associated with expanded CSF spaces, using a 2-component (gray matter + white matter versus CSF) approach to determine CSF factors ranging from 0 to 1 (no atrophy).²²

We hypothesized that *in vivo* kinetics for [¹¹C]β-CFT would be more reversible for TBI subjects (relative to controls), in part, because DA clearance kinetics are altered in experimental TBI.^{5,6} Several analysis methods were investigated to address the range of uptake kinetics observed for [¹¹C]β-CFT. These included (1) arterial-based methods: two-tissue compartment model (k1 to k4, blood volume = 0.05) and Logan graphical analysis²³ and also (2) reference tissue-based methods: simplified reference tissue method (SRTM2)²⁴ and Logan. [¹¹C]RAC data were analyzed as previously described.¹² The cerebellum was used as reference region for both radioligands (i.e. representative of nondisplaceable tissue uptake).^{25,26} DAT/D2R binding were assessed using the nondisplaceable binding potential (BP_{ND}) outcome, BP_{ND} = DVR - 1, where DVR (distribution volume ratio) is the ratio of the regional volume of distribution value (V_T) to that determined for the cerebellar reference region (V_{ND}).²⁵ Other SRTM2 parameters examined (before CSF or age corrections) were the apparent clearance (k_{2a}, per minute) and the ratio of relative radiotracer delivery in a region of interest relative to that in the reference region (R₁).

Statistical Analysis and Primary Outcomes

Descriptive statistics were performed using SPSS v19 and Excel 2010. Summary statistics for continuous variables were computed. Means, standard error of the mean (s.e.m.), and standard deviation were generated for all striatal ROIs. A two-sided hypothesis (*P*-value ≤ 0.05) was used for all analyses. Regional BP_{ND} values for grouped caudate, putamen, and striatum were the primary dependent variables. Normality tests for BP_{ND} were evaluated using group-based statistics, and none violated assumptions. As there were no hypotheses surrounding lateralization of findings or specific reward pathways, hemisphere specific, and other subregion ROIs were not explored. Pearson's correlation analysis was used to compare the consistency of ROI BPs generated using arterial-based Logan (LoganART), reference tissue-based Logan (LoganREF), and SRTM2 methods. Group differences for continuous variables were examined using independent samples *t*-tests. To examine the influence of genetic variants on regional BPs, TBI subjects and controls were grouped on the basis of

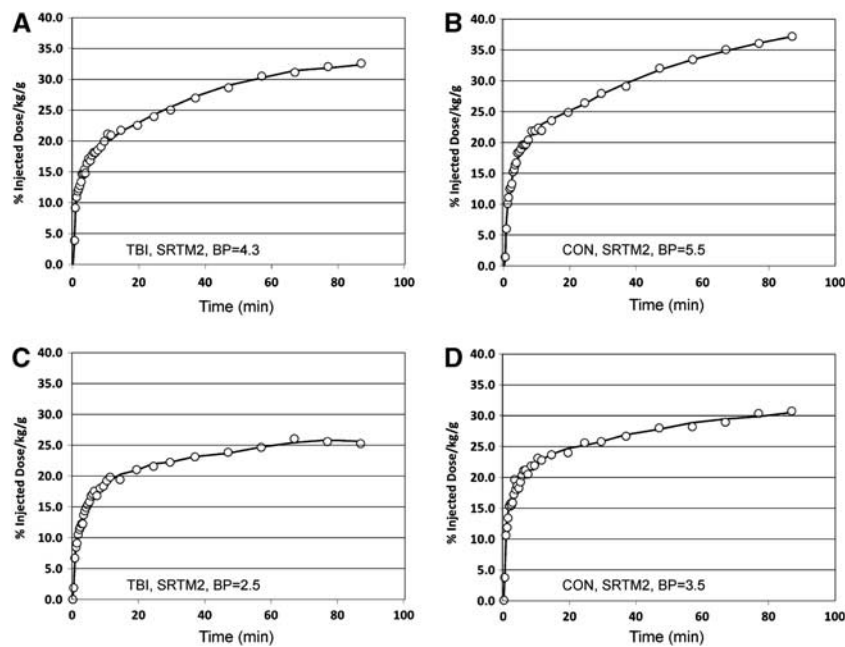


Figure 1. Putamen [^{11}C] βCFT time activity curves (open circles) that depict the high (top) and low (bottom) ranges of [^{11}C] βCFT binding in TBI (A/C) and control (B/D) subjects. Also shown are the SRMT2 curve fits (solid lines) to the observed PET data and corresponding quantitative binding potential (BP) values. PET, positron emission tomography; TBI, traumatic brain injury.

presence or absence of the variant (i.e. DAT 9-carriers versus DAT 10/10 homozygotes, DRD2 A1-carriers versus DRD2 A2/A2 homozygotes).

Previous literature demonstrates that striatal DAT and D2R BPs can be influenced by multiple factors, including age²⁷ and genotype.^{28,29} Controls were quasi-matched to TBI subjects enrolled on the basis of age and genotype. However, age by genotype matching was not performed. To control for age, multiple linear regression analyses were conducted to determine the main effects of genotype and injury status, after adjusting for age, on regional BP_{ND} . DAT1/DRD2 genotype effects on DAT and D2R binding were assessed using both type-I and type-III sum of squares. Interactions between age, genotype, injury status, and binding were also explored.

RESULTS

Population Demographics

The mean Glasgow Coma Score for TBI subjects was 7.3 ± 0.80 . The most common cause of injury was automobile accidents (58%). Anatomic neuroimaging results from the TBI group included diffuse axonal injury, hemorrhagic contusions, subdural hematoma, and subarachnoid hemorrhage. There were no differences between TBI subjects and controls in caffeine or alcohol use, including quantities at the time of imaging. Significantly more TBI subjects reported current tobacco use compared with controls at the time of imaging (54.5% cases versus 0% controls $P = 0.012$). No controls were on central nervous system-altering medications. Among TBI subjects, four were on antidepressants, four on amantadine, three on medication for sleep, one on galatamine, and one on klonopin.

Although controls had higher mean education levels than the TBI group (16.62 ± 0.78 versus 13.08 ± 0.58 years; $P = 0.002$), there were no genotype or age differences. However, there were significant age differences for TBI subjects on the basis of DAT1 9-allele carriage (38.60 ± 2.67 versus 25.87 ± 2.86 years; $P = 0.009$). There was a trend for an age effect among TBI subjects by DRD2 A1-carrier status (28.51 ± 3.42 versus 37.55 ± 3.33 years; $P = 0.101$). Among controls, age was also associated with presence/absence of the DAT1 9-allele (25.05 ± 2.18 versus 35.26 ± 3.52 years; $P = 0.032$).

Table 1A. PET imaging parameters (mean \pm s.d.)

Group	N	Injected dose (mCi)	P-value	Injected mass (μg)	P-value
[^{11}C]$\beta\text{-CFT}$					
TBI	11	10.59 ± 0.42	0.160	1.91 ± 0.54	0.090
Control	13	10.25 ± 0.66		1.50 ± 0.59	
[^{11}C]RAC					
TBI	11	10.38 ± 0.58	0.870	2.70 ± 0.79	0.440
Control	13	10.43 ± 0.72		2.46 ± 0.73	

TBI, traumatic brain injury.

Positron Emission Tomography Imaging and Plasma Analyses

No group differences occurred with injected dose or co-injected nonradioactive mass for either radioligand (Table 1A); although, differences for [^{11}C] $\beta\text{-CFT}$ approached trend level. Notably, the co-injected mass was 2 to 3 μg and not expected to significantly impact radioligand binding. Arterial input functions were generated for 19 subjects for both [^{11}C] $\beta\text{-CFT}$ (9 TBI; 10 control) and [^{11}C]RAC (10 TBI; 9 control), although determination of the unmetabolized fraction of [^{11}C] $\beta\text{-CFT}$ was problematic, particularly at 60 and 90 minutes because of challenges related to the extraction process. As a result, [^{11}C] $\beta\text{-CFT}$ values were not quantifiable for two subjects at 60 minutes (one TBI, one control) and data for two control subjects were fixed to the overall mean values (given no evidence of group differences in [^{11}C] $\beta\text{-CFT}$ metabolism at any time). The fractions of unmetabolized radioligand in plasma at 2, 10, 30, 60, or 90 minutes were: (1) [^{11}C] $\beta\text{-CFT}$: 0.957 ± 0.013 ($n = 17$), 0.950 ± 0.014 ($n = 17$), 0.918 ± 0.020 ($n = 17$), 0.845 ± 0.042 ($n = 15$), 0.805 ± 0.043 ($n = 15$) for (2) [^{11}C]RAC: 0.967 ± 0.016 , 0.955 ± 0.015 , 0.919 ± 0.019 , 0.847 ± 0.046 , 0.766 ± 0.070 ($n = 19$ for all), with no evidence of group differences. Polynomial smoothing was applied to the arterial data after the peak value.

Image Processing and Analyses

Similar to Ouchi *et al.*,³⁰ compartmental modeling for [¹¹C]β-CFT proved problematic, as a result of instability in k4 for slowly clearing kinetics, particularly in control subjects. This issue also contributed to variable SRTM2 results (fixed k2 to k3 region average).

Correlations between SRTM2 and LoganART BP_{ND} were stronger across ten TBI subjects for the three ROIs (*r*=0.917 to 0.963; *P*≤0.001, all comparisons) versus the nine controls (*r*=0.224 to 0.838; *P*=0.533 to 0.002), consistent with more reversible TBI kinetics. The BP_{ND} correlations between LoganART and LoganREF also were stronger for TBI subjects across ROIs (*r*=0.927 to 0.978; *P*<0.001, all comparisons) than for slower clearing controls (*r*=0.452 to 0.770; *P*=0.190 to 0.009) (Table 1B). [¹¹C]β-CFT-BP_{ND} was higher for LoganART and SRTM2 than LoganREF BP_{ND} for both groups. In contrast, regional [¹¹C]RAC-BP_{ND} was similar in value and significantly correlated across analysis methods for both TBI and control subjects, consistent with reversible kinetics in both groups (Table 1B). Together, the correlational results are consistent with injury-specific DAT-binding affinity differences leading to more reversible [¹¹C]β-CFT kinetics for TBI subjects than controls. These correlational results were very similar with/without CSF correction (further description below). The statistical analyses were focused on regional [¹¹C]β-CFT and [¹¹C]RAC SRTM2 BP_{ND} values.

Examination of the SRTM2 R₁, as a proxy of relative blood flow, did not reveal significant TBI/control differences for either radiotracer, across ROIs (two-sided *t*-test, *P*<0.05), although R₁ was slightly lower for controls ([¹¹C]β-CFT: 2 to 6% and [¹¹C]RAC: 1 to 3%). For both radiotracers, the lowest average R₁ (*n*=23) was

observed in caudate (~0.8, ROI with greatest CSF dilution (see below)), relative to the putamen and ventral striatum (~0.9, rarely exceeding 1.0).

Cerebrospinal fluid correction values for TBI subjects were lower than for controls but reflective of minor atrophy in the putamen and ventral striatum (>0.98) and greater atrophy in caudate (0.86±0.02). Among TBI subjects, CSF correction values by genotype were similar (data not shown). Therefore, BP_{ND} data were corrected for atrophy-related CSF dilution, presumably resulting from the TBI, and data are reported with and without CSF correction (Tables 1C and 1D). We postulated that atrophy effects associated with tissue loss might accentuate decreases in [¹¹C]β-CFT-BP_{ND} post-injury. However, without CSF correction, injury induced and/or genetic effects regulating BP_{ND} or extracellular DA levels might be missed. As expected, DAT reductions were larger when assessing BP_{ND} without CSF correction, primarily in the caudate, compared with CSF-corrected data (Tables 1C and D). Mean injury-induced [¹¹C]β-CFT-BP_{ND} reductions in caudate, using CSF adjusted data, were ~90% of that observed with uncorrected BP_{ND} data. [¹¹C]β-CFT-BP_{ND} in other regions, and [¹¹C]RAC-BP_{ND}, were similar with/without CSF correction. Upon CSF correction, data still showed injury and genotype influences on BP_{ND}, and CSF-corrected results, using SRTM2, are presented for bivariate and multivariate analyses that incorporated genotype, age, and injury status.

Injury Effects on Striatal DAT and DRD2 Binding Potentials

Lower DAT [¹¹C]β-CFT-BP_{ND} was observed in TBI subjects than controls. Significant injury group differences were observed in the caudate, putamen, and ventral striatum (*P*≤0.026) for SRTM2 BP_{ND} with/without CSF correction, (Table 1C). Figure 1 shows example [¹¹C]β-CFT time-activity curves with corresponding SRTM2 model fits for high and low putamen binding in TBI subjects and controls. The rank order of apparent [¹¹C]β-CFT clearance (*k*_{2a}) for these four subjects was TBI_{Low} *k*_{2a}=0.0149 per minute, TBI_{High} *k*_{2a}=0.0112 per minute, Con_{Low} *k*_{2a}=0.0107 minute, Con_{High} *k*_{2a}=0.0081 minute consistent with greater apparent clearance for TBI subjects. Logan [¹¹C]β-CFT-BP_{ND} results were consistent with these findings but of lower statistical significance, and loss of statistical significance in ventral striatum (Table 1C). Traumatic brain injury subjects exhibited higher [¹¹C]RAC-BP_{ND} (versus controls) in ventral striatum for DRD2, but only at marginal statistical significance for Logan BP_{ND} and SRTM2 BP_{ND} (Table 1C).

Influence of Genetic Variants on DAT and DRD2 Binding

Figures 2A and B show a color map representation of dynamic PET images for [¹¹C]β-CFT and [¹¹C]RAC-BP_{ND} in the ventral striatum. Figures 2C and D show similar PET images for putamenal [¹¹C]β-CFT-BP_{ND} when comparing 9-allele carriers with 10/10 homozygotes and also when comparing A2/A2 homozygotes with A1-carriers among TBI subjects and controls. Figures 2A and C show representative images of reduced [¹¹C]β-CFT-BP_{ND} with TBI versus controls and also for 9-allele versus 10/10 carriers with TBI. Figure 2B shows increased [¹¹C]RAC-BP_{ND} with TBI versus controls, particularly with A1-carriers compared with A2/A2 homozygotes with TBI. Figure 2D shows reduced [¹¹C]β-CFT-BP_{ND} in A2/A2 homozygotes versus A1-carriers among TBI subjects.

Bivariate analyses (CSF-corrected BP_{ND}). Bivariate comparisons for Cerebrospinal fluid-corrected BP_{ND} in the caudate, putamen, and ventral striatum are shown in Figure 3. When TBI subjects were grouped on the basis of DAT 9-allele status, 9-carriers had lower [¹¹C]β-CFT-BP_{ND} in caudate (*P*=0.011) and putamen (*P*=0.009) ROIs compared with non-carriers. Also, A1-carriers with TBI had higher [¹¹C]β-CFT-BP_{ND} in the putamen compared with A2/A2 homozygotes (*P*=0.034). Among controls, there were no regional

Table 1B. Pearson correlation coefficients (*r*)—CSF corrected

	TBI	P-value	Control	P-value
<i>Raclopride correlations</i>				
LoganART versus LoganREF				
CAG	0.996	<0.001	0.999	<0.001
PUG	0.995	<0.001	0.999	<0.001
VSG	0.997	<0.001	0.999	<0.001
LoganART versus STRM2				
CAG	0.946	<0.001	0.993	<0.001
PUG	0.957	<0.001	0.972	<0.001
VSG	0.978	<0.001	0.993	<0.001
LoganREF versus SRTM2				
CAG	0.977	<0.001	0.990	<0.001
PUG	0.976	<0.001	0.980	<0.001
VSG	0.982	<0.001	0.994	<0.001
<i>CFT Correlations</i>				
LoganART versus LoganREF				
CAG	0.963	<0.001	0.537	0.110
PUG	0.927	<0.001	0.452	0.190
VSG	0.978	<0.001	0.770	0.009
LoganART versus SRTM2				
CAG	0.944	<0.001	0.224	0.533
PUG	0.917	0.001	0.716	0.020
VSG	0.963	<0.001	0.838	0.002
LoganREF versus SRTM2				
CAG	0.990	<0.001	0.726	0.005
PUG	0.953	<0.001	0.570	0.042
VSG	0.959	<0.001	0.607	0.028

CSF, cerebrospinal fluid; LoganART, arterial-based Logan; LoganREF; reference tissue-based Logan. Very similar results were obtained without CSF correction (data not shown). Bold entries are made for *P*-values representing comparisons that are statistically significant.

Table 1C. Bivariate associations with injury status with CSF correction

C-11-β-CFT	LoganREF			LoganART			SRTM2		
	TBI (N = 11)		Control (N = 13)	TBI (N = 9)		Control (N = 10)	TBI (N = 11)		Control (N = 13)
	Mean BP ± s.e.m.	Mean BP ± s.e.m.	P-value	Mean BP ± s.e.m.	Mean BP ± s.e.m.	P-value	Mean BP ± s.e.m.	Mean BP ± s.e.m.	P-value
CSF corrected									
Caudate	2.342 ± 0.200	2.693 ± 0.118	0.131	4.256 ± 0.532	5.677 ± 0.272	0.025	3.740 ± 0.409	5.058 ± 0.165	0.010^a
Putamen	2.138 ± 0.106	2.611 ± 0.098	0.003	3.617 ± 0.299	5.332 ± 0.313	0.001	3.175 ± 0.193	4.666 ± 0.172	< 0.001
Striatum	2.138 ± 0.127	2.331 ± 0.109	0.256	3.677 ± 0.345	4.354 ± 0.276	0.141	3.141 ± 0.225	3.918 ± 0.232	0.026
C-11-Raclopride	LoganREF			LoganART			SRTM2		
	TBI (N = 12)		Control (N = 13)	TBI (N = 10)		Control (N = 9)	TBI (N = 12)		Control (N = 13)
	Mean BP ± s.e.m.	Mean BP ± s.e.m.	P-value	Mean BP ± s.e.m.	Mean BP ± s.e.m.	P-value	Mean BP ± s.e.m.	Mean BP ± s.e.m.	P-value
CSF Corrected									
Caudate	2.688 ± 0.116	2.556 ± 0.080	0.392	2.693 ± 0.124	2.625 ± 0.100	0.679	2.770 ± 0.118	2.627 ± 0.072	0.315 ^a
Putamen	2.777 ± 0.100	2.864 ± 0.073	0.486	2.827 ± 0.115	2.898 ± 0.091	0.640	2.800 ± 0.095	2.905 ± 0.072	0.379
Striatum	2.769 ± 0.089	2.491 ± 0.101	0.052	2.798 ± 0.088	2.477 ± 0.117	0.041	2.760 ± 0.862	2.493 ± 0.107	0.068

CSF, cerebrospinal fluid; LoganART, arterial-based Logan; LoganREF; reference tissue-based Logan; TBI, traumatic brain injury. ^aEqual variance not assumed. Bold entries are made for P-values representing comparisons that are statistically significant.

Table 1D. Bivariate associations with injury status without CSF correction

C-11-β-CFT	LoganREF			LoganART			SRTM2		
	TBI (N = 11)		Control (N = 13)	TBI (N = 9)		Control (N = 10)	TBI (N = 11)		Control (N = 13)
	Mean BP ± s.e.m.	Mean BP ± s.e.m.	P-value	Mean BP ± s.e.m.	Mean BP ± s.e.m.	P-value	Mean BP ± s.e.m.	Mean BP ± s.e.m.	P-value
No CSF corrected									
Caudate	1.931 ± 0.170	2.414 ± 0.113	0.023	3.606 ± 0.463	5.149 ± 0.263	0.008	3.154 ± 0.346	4.609 ± 0.185	0.001
Putamen	2.190 ± 0.101	2.655 ± 0.094	0.003	3.695 ± 0.296	5.384 ± 0.327	0.001	3.244 ± 0.187	4.839 ± 0.178	< 0.001
Striatum	2.149 ± 0.119	2.360 ± 0.105	0.196	3.689 ± 0.333	4.375 ± 0.280	0.131	3.153 ± 0.214	3.965 ± 0.239	0.021
C-11-Raclopride	LoganREF			LoganART			SRTM2		
	TBI (N = 12)		Control (N = 13)	TBI (N = 10)		Control (N = 9)	TBI (N = 12)		Control (N = 13)
	Mean BP ± s.e.m.	Mean BP ± s.e.m.	P-value	Mean BP ± s.e.m.	Mean BP ± s.e.m.	P-value	Mean BP ± s.e.m.	Mean BP ± s.e.m.	P-value
No CSF Corrected									
Caudate	2.225 ± 0.092	2.300 ± 0.084	0.559	2.242 ± 0.099	2.337 ± 0.105	0.522	2.297 ± 0.094	2.354 ± 0.077	0.637
Putamen	2.835 ± 0.099	2.911 ± 0.066	0.525	2.893 ± 0.116	2.292 ± 0.088	0.814	2.858 ± 0.094	2.953 ± 0.065	0.409
Striatum	2.783 ± 0.093	2.522 ± 0.099	0.096	2.817 ± 0.098	2.492 ± 0.119	0.049	2.774 ± 0.088	2.524 ± 0.107	0.087

CSF, cerebrospinal fluid; LoganART, arterial-based Logan; LoganREF; reference tissue-based Logan; TBI, traumatic brain injury. Bold entries are made for P-values representing comparisons that are statistically significant.

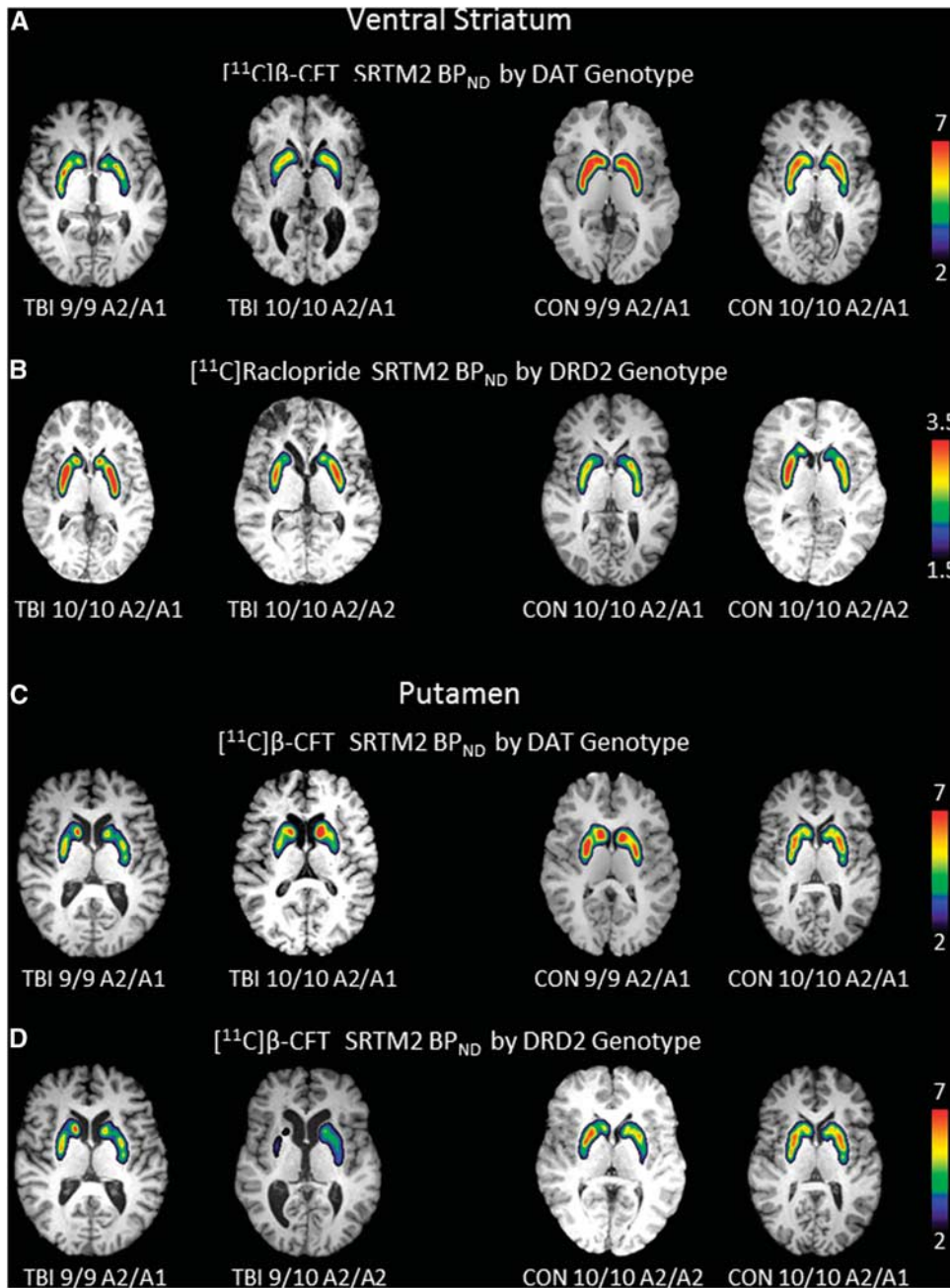


Figure 2. Images depict regional binding for [^{11}C] β -CFT and [^{11}C]raclopride based on SRTM2 analysis using cerebellum as reference region for a single slice through the ventral striatum (**A/B**) and putamen (**C/D**) in the axial plane overlaid onto high resolution anatomic MRI. (**A**) Shows a representative image of the ventral striatum and DAT binding in persons with DAT1 genotype 9/9 and DAT1 genotype 10/10 while keeping the DRD2 constant for the A2/A1 genotype in TBI (left two panels) and controls (right two panels). Panel **B** shows a representative image through the ventral striatum of DRD2 binding in persons with DRD2 genotype A2/A1 and DRD2 genotype A2/A2 while keeping DAT constant for the 10/10 genotype in TBI (left two panels) and controls (right two panels). Panel **C** shows a representative image of the putamen and DAT binding in persons with DAT1 genotype 9/9 and DAT1 genotype 10/10 while keeping the DRD2 constant for the A2/A1 genotype in TBI (left two panels) and controls (right two panels). Panel **D** shows a representative image of the putamen and DAT binding in persons with DRD2 genotype A1/A2 and A2/A2 while keeping the DAT1 genotype constant for the 10/10 genotype in TBI (left two panels) and controls (right two panels). Note: TBI 9/10 A2/A2 scale was 1.5 to 6. CON, control; DAT, dopamine transporter; MRI, magnetic resonance imaging; TBI, traumatic brain injury.

[^{11}C] β -CFT- BP_{ND} differences with the caudate and putamen based on DAT 9-allele status. However, A1-carriers had higher BP_{ND} in the ventral striatum compared with A2/A2 homozygotes ($P=0.014$; Table 2A). Also, an injury-specific genetic relationship was observed for DAT binding, where 9-carriers with TBI had lower

caudate and putamen ($P<0.001$), and striatum ($P=0.046$) BP_{ND} than 9-carrier controls. There were no regional injury group differences in [^{11}C] β -CFT- BP_{ND} among DAT1 10/10 carriers. However, TBI A2/A2 subjects had lower [^{11}C] β -CFT- BP_{ND} in caudate and putamen ($P<0.001$) versus A2/A2 controls. For

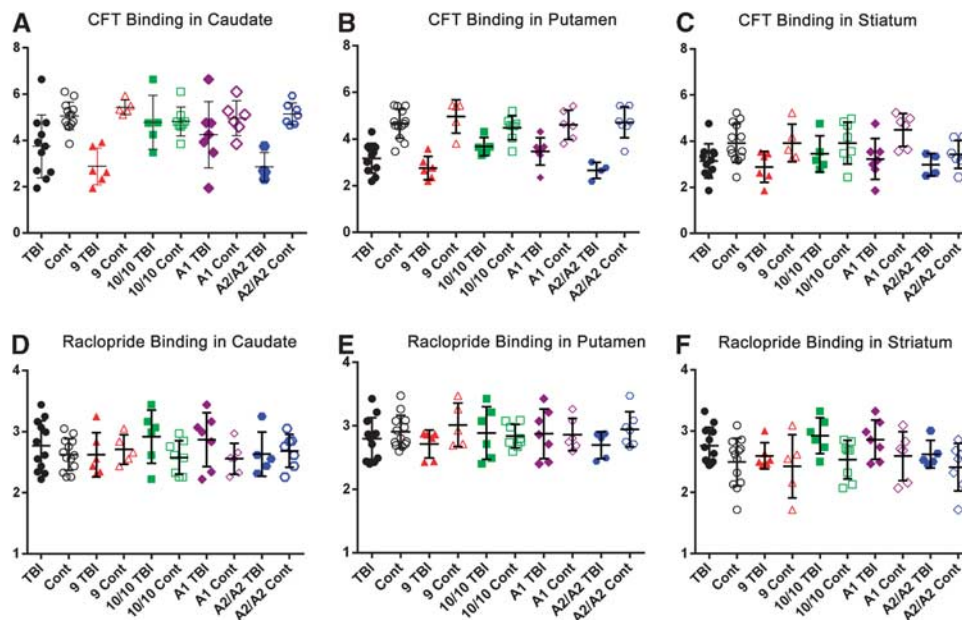


Figure 3. Column scatter graphs showing mean \pm s.d. binding potential for CFT (**A–C**) and Raclopride (**D–F**) in the caudate (**A, D**), putamen (**B, E**), and striatum (**C, F**) with superimposed individual binding potential values by injury, DAT genotype, and DRD2 genotype groupings. Cont, control; TBI, traumatic brain injury.

Table 2A. Bivariate analysis—Influence of DAT genotype on binding potential

DAT genotype	CSF corrected SRTM2 CFT: TBI			CSF corrected SRTM2 CFT: control		
	9-carriers (N = 6)		P-value	9-carriers (N = 5)		P-value
	Mean BP \pm s.e.m.	Mean BP \pm s.e.m.		Mean BP \pm s.e.m.	Mean BP \pm s.e.m.	
Caudate	2.877 \pm 0.324	4.777 \pm 0.521	0.011	5.429 \pm 0.139	4.826 \pm 0.222	0.073
Putamen	2.760 \pm 0.203	3.674 \pm 0.173	0.009	4.966 \pm 0.319	4.478 \pm 0.182	0.178
Striatum	2.884 \pm 0.272	3.449 \pm 0.342	0.229	3.922 \pm 0.367	3.916 \pm 0.320	0.991
DRD2 genotype	A1-carriers (N = 7)		P-value	A2/A2 (N = 5)		P-value
	A1-carriers (N = 6)			A2/A2 (N = 7)		
	Mean BP \pm s.e.m.	Mean BP \pm s.e.m.	Mean BP \pm s.e.m.	Mean BP \pm s.e.m.	Mean BP \pm s.e.m.	Mean BP \pm s.e.m.
Caudate	4.249 \pm 0.541	2.850 \pm 0.311	0.101	4.956 \pm 0.307	5.145 \pm 0.118	0.591
Putamen	3.471 \pm 0.222	2.657 \pm 0.172	0.034	4.610 \pm 0.256	4.713 \pm 0.250	0.779
Striatum	3.233 \pm 0.334	2.980 \pm 0.243	0.614	4.491 \pm 0.291	3.428 \pm 0.231	0.014

BP, binding potential; CSF, cerebrospinal fluid; DAT, dopamine transporter; DRD2, D2 receptor gene; TBI, traumatic brain injury. Bold entries are made for P-values representing comparisons that are statistically significant.

A1-carriers, TBI subjects had lower [^{11}C]-CFT-BP_{ND} in putamen ($P = 0.006$) and striatum ($P = 0.018$) than controls. Together, bivariate analysis shows that [^{11}C]-CFT-BP_{ND} reductions among TBI subjects were associated with both DAT1 and DRD2 genotype.

When evaluating the DRD2 A1 variant allele, there was no difference in [^{11}C]-RAC-BP_{ND} (Table 2B) with TBI or control groups. Also, there was no injury effect for DRD2 genotype. When comparing TBI subjects, DAT1 10/10 homozygotes had marginally significant increases in [^{11}C]-RAC-BP_{ND} in the ventral striatum compared with 9-carriers ($P = 0.052$) (Table 2B). DAT1 10/10 subjects with TBI had higher [^{11}C]-RAC-BP_{ND} than controls ($P = 0.036$), however, [^{11}C]-RAC-BP_{ND} were similar for injured and control DAT1 9-carriers.

Multivariate analysis. Multivariate analyses were conducted to examine (1) age and genotype influences on [^{11}C]-CFT and [^{11}C]-RAC-BP_{ND} for the caudate, putamen, and striatum among TBI subjects (Table 3) and (2) age (and genotype) specific injury influences on [^{11}C]-CFT and [^{11}C]-RAC-BP_{ND} for these regions (Tables 4A and B).

Among TBI subjects, age effects on [^{11}C]-RAC-BP_{ND} were significant for striatum ($P = 0.023$), and the association with [^{11}C]-CFT-BP_{ND} approached significance in caudate ($P = 0.062$). When controlling both age and genotype, age effects on [^{11}C]-CFT-BP_{ND} were not significant in any region, whereas DAT1 genotype remained significant in the caudate ($P = 0.032$) and putamen ($P = 0.009$), showing that the primary relationship with

Table 2B. Bivariate analysis—Influence of DRD2 genotype on binding potential

DRD2 genotype	CSF corrected SRTM2 raclopride: TBI			CSF corrected SRTM2 raclopride: control				
	A1-carriers (N = 7)	A2/A2 (N = 5)		A1-carriers (N = 6)	A2/A2 (N = 7)			
	Mean BP ± s.e.m.	Mean BP ± s.e.m.	P-value	Mean BP ± s.e.m.	Mean BP ± s.e.m.	P-value		
Caudate	2.867 ± 0.167	2.634 ± 0.162	0.357	2.557 ± 0.104	2.686 ± 0.102	0.398		
Putamen	2.874 ± 0.147	2.696 ± 0.096	0.379	2.861 ± 0.104	2.943 ± 0.106	0.595		
Striatum	2.859 ± 0.121	2.622 ± 0.101	0.187	2.591 ± 0.162	2.410 ± 0.147	0.424		
DAT genotype	9-carriers (N = 6)		10/10 (N = 6)		9-carriers (N = 5)		10/10 (N = 8)	
	Mean BP ± s.e.m.		Mean BP ± s.e.m.		Mean BP ± s.e.m.		Mean BP ± s.e.m.	
	P-value		P-value		P-value		P-value	
Caudate	2.662 ± 0.147		2.918 ± 0.147		2.708 ± 0.108		2.576 ± 0.097	
Putamen	2.713 ± 0.089		2.886 ± 0.089		3.013 ± 0.154		2.838 ± 0.066	
Striatum	2.595 ± 0.087		2.925 ± 0.087		2.426 ± 0.232		2.536 ± 0.111	

BP, binding potential; CSF, cerebrospinal fluid; DAT, dopamine transporter; DRD2, D2 receptor gene; TBI, traumatic brain injury. ^aEqual variance not assumed.

Table 3. Multivariate analysis—Age effects on binding among TBI subjects

Variable	Caudate—CFT: R ² = 0.588		Putamen—CFT: R ² = 0.673		Striatum—CFT: R ² = 0.285	
	Estimate	P-value	Estimate	P-value	Estimate	P-value
Intercept	3.347	0.052	2.667	0.003	2.228	0.070
Age	0.016	0.338	0.043	0.127	0.052	0.264
DAT	-2.838	0.032	-1.575	0.009	-1.366	0.123
Variable	Caudate—RAC: R ² = 0.143		Putamen—RAC: R ² = 0.146		Striatum—RAC: R ² = 0.370	
	Estimate	P-value	Estimate	P-value	Estimate	P-value
Intercept	2.856	<0.001	3.233	<0.001	3.157	<0.001
Age	0.002	0.906	-0.013	0.413	-0.009	0.483
DRD2	-0.326	0.373	-0.003	0.992	-0.216	0.346

DAT, dopamine transporter; DRD2, D2 receptor gene; TBI, traumatic brain injury. Bold entries are made for P-values representing comparisons that are statistically significant.

Table 4A. Multivariate analysis—age controlled injury effects on CFT/Raclopride binding

Variable	Caudate—CFT: R ² = 0.494		Putamen—CFT: R ² = 0.668		Striatum—CFT: R ² = 0.225	
	Estimate	P-value	Estimate	P-value	Estimate	P-value
Intercept	5.463	<0.001	4.024	<0.001	3.563	<0.001
Age	-0.054	0.012	-0.027	0.054	-0.013	0.466
Injury status	1.300	0.002	1.482	< 0.001	0.773	0.029
Variable	Caudate—RAC: R ² = 0.172		Putamen—RAC: R ² = 0.255		Striatum—RAC: R ² = 0.209	
	Estimate	P-value	Estimate	P-value	Estimate	P-value
Intercept	3.193	<0.001	3.280	<0.001	3.102	<0.001
Age	-0.013	0.080	-0.015	0.018	-0.011	0.173
Injury status	-0.155	0.245	0.092	0.393	-0.276	0.055

DAT, dopamine transporter; DRD2, D2 receptor gene. Bold entries are made for P-values representing comparisons that are statistically significant.

Table 4B. Multivariate analysis—Age controlled injury effects among genotype groups

Variable	Caudate—9-carriers CFT: $R^2 = 0.857$		Putamen—9-carriers CFT: $R^2 = 0.668$		Striatum—9-carriers CFT: $R^2 = 0.379$	
	Estimate	P-value	Estimate	P-value	Estimate	P-value
Intercept	1.427	0.310	1.762	0.216	2.459	0.177
Age	0.038	0.294	0.026	0.461	0.011	0.801
Injury status	3.061	0.001	2.556	0.002	1.187	0.148
Variable	Caudate—A2/A2 carriers CFT: $R^2 = 0.845$		Putamen—A2/A2 carriers CFT: $R^2 = 0.826$		Striatum—10/10 carriers RAC: $R^2 = 0.566$	
	Estimate	P-value	Estimate	P-value	Estimate	P-value
Intercept	2.571	0.027	3.918	0.003	3.593	<0.001
Age	0.008	0.766	-0.034	0.196	-0.026	0.059
Injury status	2.347	<0.001	1.820	0.001	-0.156	0.365

DAT, dopamine transporter. Bold entries are made for *P*-values representing comparisons that are statistically significant.

[¹¹C]β-CFT-BP_{ND} is DAT1 genotype. When controlling for age, there were no regional differences in [¹¹C]RAC-BP_{ND} among TBI subjects based on either DRD2 genotype (Table 3).

Multivariate analysis assessing injury status and age effects (Table 4A) on BP_{ND}, showed that age was associated with [¹¹C]β-CFT-BP_{ND} in caudate ($P=0.012$) and was marginally associated with [¹¹C]β-CFT-BP_{ND} in the putamen ($P=0.054$) and with [¹¹C]RAC-BP_{ND} in the putamen ($P<0.018$). Age-adjusted [¹¹C]β-CFT-BP_{ND} reductions with TBI status were significant in the caudate, putamen, and striatum ($P<0.03$, all comparisons). Age-adjusted [¹¹C]RAC-BP_{ND} was marginally higher in ventral striatum ($P=0.055$). Age-adjusted effects of injury status within specific genotype groups was also assessed (Table 4B). Among 9-carriers, reduced [¹¹C]β-CFT-BP_{ND} occurred in the caudate and putamen ($P\leq 0.002$). Also, A2/A2 homozygotes with TBI had lower BP_{ND} compared with A2/A2 controls in the caudate and putamen ($P\leq 0.001$). However, DAT1 genotype did not impact [¹¹C]RAC-BP_{ND}.

DISCUSSION

Clinical research exploring DA deficits and dysfunction in TBI is limited, but our findings provide additional support for DA system dysfunction after severe TBI. Similar to previous reports using SPECT,⁴ our results showed lower DAT binding after severe TBI. Although the cohort size is small for genotype stratification, genetic variation in (1) the SLC6A3 gene promoter region variable number of tandem repeat and (2) the Taq1A restriction fragment length polymorphism of the DRD2 gene was associated with regional DAT binding and was injury specific. Decreased [¹¹C]β-CFT-BP_{ND} occurred in DAT 9-carriers and A2/A2 homozygotes with TBI in the caudate and putamen. There was higher overall D2R binding in the ventral striatum in the TBI group versus controls, yet this effect was not specific to DRD2/DAT1 genotype. Increased D2R-BP_{ND} with [¹¹C]RAC post injury may reflect a hypodopaminergic environment, with less competitive binding from endogenous DA and/or D2 membrane receptor upregulation/hypersensitization resulting from decreased DA availability. Similarly, injury-specific decreases with membrane-bound DAT may be a compensatory response to reduce DA reuptake, enhance DA availability, and promote DA transmission in a low DA environment. Perhaps A2/A2 homozygotes with TBI may better regulate DAT trafficking, via autoreceptor modulation, resulting in decreased DAT expression associated with reduced [¹¹C]β-CFT-BP_{ND}. To our knowledge, this is the first PET study directly assessing DA receptor/protein function after TBI and linking genetic variation to DA transmission after TBI.

Previous work demonstrates lower DAT/D2R binding in subjects having very severe TBI, and associated disorders of consciousness,

compared with controls using single-photon emission tomography.⁴ Although decreased DAT binding occurs in our study, the magnitude of reductions noted in their population (~45% of controls) was larger than our study (~68% to 80% of control CSF-corrected comparison). Binding reductions in our study were slightly larger when data were not corrected for expansion of the CSF compartment, particularly in the caudate; injury-induced DAT-binding reductions after CSF correction were ~92.6% of the magnitude of DAT reductions observed without correction. Although D2R binding was decreased post injury in the Donnemiller⁴ study, [¹¹C]RAC-BP_{ND} in ventral striatum was marginally increased in our study, despite minimal CSF dilution differences in this region. We speculate that there is less competitive binding from endogenous DA and/or D2 membrane receptor upregulation/hypersensitization resulting from decreased DA availability in our study. However, increased injury severity (vegetative or akinetic state) for subjects in the Donnemiller⁴ study may also contribute to the study-specific trends with [¹¹C]RAC binding. Also, subjects with very severe TBI in this previous report may have had more nigral-striatal fiber loss, leading to decreased DAT and D2R binding compared with our study. However, frank dopaminergic fiber loss is not robust in the experimental literature, where nigral tyrosine hydroxylase staining is modestly increased after moderate-severe CCI,² and striatal vesicular monoamine transporter and tyrosine hydroxylase expression remain largely unchanged.^{5,6} Alternatively, this literature supports the concept of striatal DA transmission dysfunction after TBI leading to a functional hypodopaminergic state.² Cerebrospinal fluid-corrected comparisons in our population more likely generated BP_{ND} values reflecting regulatory changes in DAT/D2R binding in the context of a functional hypodopaminergic state as opposed to reflecting primarily DA fiber loss.

The SRTM2 BP_{ND} was used as the primary outcome, after evaluation of several methods. The [¹¹C]β-CFT kinetics observed with TBI (greater clearance) and control (greater accumulation) subjects, although [¹¹C]RAC analyses were straightforward with arterial input function determination and reversible kinetics for both groups. Complexities with [¹¹C]β-CFT analyses were consistent with early observations.^{21,30,31} Relationships between arterial and reference tissue results increased our confidence in the noninvasive reference methods that allowed us to include all available subjects, although these methods are vulnerable to well-known biases²³ when linear regression and steady-state assumptions are not well satisfied. The SRTM2 method performed stably yielding BP_{ND} measures generally consistent with arterial-based and reference Logan methods, although BP_{ND} magnitudes differed between the modeling and regression methods. Notably, no

groups differed in the later summed cerebellar reference tissue kinetics (e.g., %ID*kg/g) for either tracer. Descriptive analyses comparing SRTM2, LoganART, and LoganREF yielded lower correlations for [¹¹C]β-CFT in controls than for TBI, consistent with injury-specific DAT-binding affinity differences leading to greater apparent [¹¹C]β-CFT clearance for TBI subjects that could be reflective of a higher dissociation constant. Injury-induced changes in DAT expression/function are supported in experimental TBI, where DA clearance patterns reflect changes in membrane-bound DAT expression/trafficking behavior as well as function (e.g., binding affinity).⁶

Decreased striatal expression of the fully glycosylated form of DAT, required for membrane expression, has been repeatedly observed after CCI injury using western blot.^{5,6} However, in striatal synaptosomal preparations, membrane-bound DAT expression is increased chronically after CCI compared with controls, indicating that overall reductions in fully glycosylated DAT may be primarily because of decreased extra-synaptic DAT expression.⁶ Decreased DAT binding in this clinical population supports overall decreases in membrane-bound DAT noted in CCI. DAT binding is subject to rapid regulatory changes affecting membrane expression.³² Although some DA fiber loss may occur, reduced DAT expression post TBI possibly may compensate for a hypodopaminergic environment after TBI.² Presynaptic D2 auto-receptors regulating DAT expression and trafficking can be susceptible to injury.³³ Thus, D2 autoreceptor function post injury may facilitate reduced DAT binding in the caudate and putamen, where DAT reductions are most notable.

Striatal DA neurotransmission after CCI suggests impaired D2R autoreceptor regulation of DA release that normalizes with daily MPD treatment, providing indirect evidence that striatal basal DA levels are decreased with TBI.⁶ Evidence for a hypodopaminergic environment in unilateral Parkinson's disease lesion models show that reduced dopaminergic inputs result in a hypodopaminergic environment and increased post-synaptic striatal D2R expression/sensitization that mediates rotational behavior when paired with potent D2 agonists like amphetamine.³⁴ After unilateral CCI, some rats display rotational behavior 2 weeks after amphetamine challenge,⁵ supporting the concept of a hypodopaminergic environment, and possibly increased post-synaptic D2R expression, after CCI. In contrast, persistently lower D2R binding occurs in long-term cocaine abusers³⁵ where reward-like behaviors stimulate DA transmission and result in decreased D2R expression. In our study, evidence of a hypodopaminergic state in ventral striatum is supported by increased [¹¹C]RAC-BP_{ND}. Variable radiotracer competition with endogenous DA levels is expected because of relatively low affinity of [¹¹C]RAC for D2R. Interestingly, increased D2R binding post TBI did not occur in the caudate or putamen, where DAT-binding reductions are more prominent. Conversely, ventral striatum had minimal injury-induced DAT reductions with increased D2R binding, providing indirect evidence that regional DAT reductions may facilitate normalized DA neurotransmission after TBI.

Variation in the DAT SLC6A3 gene promoter region variable number of tandem repeats is associated with attention deficit hyperactivity disorder. Studies show that 10/10 homozygotes have increased attention deficit hyperactivity disorder risk.⁹ Also, DAT 10/10 homozygosity has been linked with higher DAT binding,²⁸ yet others suggest 9-carriers have higher binding.²⁹ Our study showed no significant binding differences based on DAT1 genotype among controls, further adding to the range of literature on genetic variability and DAT binding in uninjured populations. However, with differences of 9 to 22% for genotype related changes in binding, the sample size of our control cohort may be underpowered to discriminate genotype effects.

A1-carriage for the DRD2 Taq1 restriction fragment length polymorphism is associated with a low density of striatal D2 receptors.³⁶ Decreased striatal metabolism is also noted in

A1-carriers compared with A2/A2 homozygotes.³⁷ Although marginally significant injury-associated increases in [¹¹C]RAC-BP_{ND} were observed, A1-carriers did not have different [¹¹C]RAC-BP_{ND} than A2/A2 homozygotes in the ventral striatum post TBI. However, A2/A2 homozygotes with TBI had lower DAT binding, suggesting that genetic variability for DRD2 might differentially involve D2 autoreceptor interactions with DAT versus post-synaptic D2R upregulation associated with a functionally low DA state. Although this association is subject to future validation studies, the literature does not define if/how the Taq1 variant is differentially linked to pre/post-synaptic D2 receptor expression. Recent work identifies single-nucleotide polymorphisms associated specifically with presynaptic D2R expression^{38,39} and mRNA stability,⁴⁰ some of which are linked to decreased striatal D2R/DAT binding using SPECT,³⁹ findings which warrant further investigation of genetically mediated D2 autoreceptor—DAT regulation in the context of TBI.

Our TBI population included only men, so sex-linked differences in DAT/DRD2 binding post TBI were not a factor. Aging-related decrements in striatal DAT binding have been reported.⁴¹ Although our subjects had a fairly narrow age range, there were age-related differences in specific genotype groups within our TBI population. Age-adjusted multivariate analysis showed that reduced DAT binding in 9-carriers with TBI versus 10/10 homozygotes were primarily due to genotype and not increased age. Similarly, decreased DAT binding among A2/A2 TBI subjects, compared with controls, were injury specific and not age related.

Although not the focus of this analysis, changes in DAT/D2R binding may have implications for cognitive performance and neurostimulant response after TBI. Positron emission tomography studies using ¹⁸F-dopa in Parkinson's disease show correlations between DAergic depletion in the caudate and neuropsychological performance. Bruck⁴² demonstrated bilateral caudate underactivity in an executive impaired subgroup of Parkinson's disease patients, suggesting a role for this region in cognition. Given our hypotheses that genotype-specific DAT regulation may be a compensatory response to improve neurotransmission, injury-specific, baseline cognitive performance associations with DAT binding also could be genotype-specific and a point of future study. Genetic associations with DAT binding were TBI-specific in our study, with the primary decreases in DAT binding attributable to reductions in 9-allele carriers. One study suggests DAT1 genotype specific differences in striatal CBF (cerebral blood flow) with MPD challenge.⁴³ Thus, genetic effects on rCBF should be considered with future pharmacogenetic imaging studies. Examination of the SRTM2 R1 (despite small samples) showed lower [¹¹C]β-CFT values for the 9-allele carriers group that ranged from 14% for caudate to 5% for putamen, whereas differences in DAT BP were much larger (40% and 25%, respectively). For [¹¹C]RAC, 9-allele carriers showed lower R₁ values of 14% for both caudate and ventral striatum and 9% for the putamen, with only marginal striatal BP differences of 11%. No R₁ differences were suggested when comparing A1 versus A2/A2 genotypes. Further, potential contributors to variation in rCBF, including age, atrophy, injury, and genotype effects, were considered and accounted for in our study design.

[¹¹C]β-CFT and [¹¹C]RAC sensitivity is low for extrastriatal ROIs. Thus, we focused only on striatal ROIs for this analysis, although frontal cortex binding reductions with Parkinson's disease have been reported.^{30,31} Reduced DAT expression in frontal cortex occurs after CCI, which may be relevant to cognitive deficits^{2,5} in future studies. Also, reports show TBI-induced epigenetic changes in the brain, including significant global hypo-methylation.⁴⁴ Changes in DNA methylation for dopaminergic genes⁴⁵ are common in schizophrenia and other psychiatric disorders. Thus, injury-induced changes in epigenetic modification, along with post-injury environmental exposure effects, may influence how genetic variation in SLC6A3 contributes to TBI-specific differences

in striatal DAT binding and could be considered with future studies.

CONCLUSIONS

There are injury-induced DAT-binding reductions in the caudate and putamen regions chronically in our sample of subjects with severe TBI, reflective of different [^{11}C] β -CFT-binding kinetics in those with TBI compared with controls. In addition, marginal increases in the ventral striatal D2R binding were observed in this region where injury-induced DAT reductions were smaller, suggesting the possibility of a hypodopaminergic environment. Our within-group genotype analysis provides initial evidence of injury-induced, genotype-specific reductions in DAT binding, particularly in the caudate and putamen chronically after TBI. We also hypothesize that genotype-specific associations with DAT binding may be compensatory in response to a low DA environment. We speculate that genotype-specific regulatory changes in DAT expression after TBI, as opposed to dopaminergic fiber loss, drive DAT changes; these findings may be linked with DAT/DRD2-specific genotype effects on DAT-D2 autoreceptor interactions. Injury-induced changes in DAT-binding affinity and expression may be responsible for overall injury-induced changes in DAT binding. However, further replication studies, as well as new studies, are warranted to focus on if/how genotype specific changes in DA receptor binding impact single use and daily treatment neurostimulant response after TBI. To address these pharmacogenetic studies, combining PET with MRI modalities, like resting state connectivity or fMRI cognitive testing paradigms, could be particularly useful. Finally, it may be useful to incorporate diffusion tensor imaging techniques with PET to establish if/how corticostriatal integrity impacts regional DAT and D2R binding and stimulant response.

DISCLOSURE/CONFLICT OF INTEREST

The authors declare no conflict of interest.

ACKNOWLEDGMENTS

The authors thank members of the PET Facility for their help with the performance of these studies, and specifically we thank Brian Lopresti for his help with the arterial input function determinations. The authors thank Sandra Deslouches for her work with genotyping. The authors also thank the volunteers for their participation in this multi-faceted study.

REFERENCES

- Crosson B, Halland K. Subcortical functions in cognition: toward a consensus. *J Int Neuropsychol Soc* 2003; **9**: 1027–1030.
- Bales J, Wagner AK, Kline AE, Dixon CE. Persistent cognitive dysfunction during rehabilitation of traumatic brain injury: towards a dopamine hypothesis. *Neurosci Biobehav Rev* 2009; **33**: 981–1003.
- Wagner AK, Ren D, Conley Y, Ma X, Kerr ME, Zafonte RD *et al*. Gender and genetic associations with CSF dopamine and metabolite production after severe TBI. *J Neurosurg* 2007; **106**: 537–547.
- Donnemiller E, Brenneis C, Wissel J, Scherfler C, Poewe W, Riccabona G *et al*. Impaired dopaminergic neurotransmission in patients with traumatic brain injury: a SPECT study using 123I-beta-CIT and 123I-IBZM. *Eur J Nucl Med* 2000; **27**: 1410–1414.
- Wagner AK, Sokoloski JE, Ren D, Chen X, Khan AS, Zafonte RD *et al*. Controlled cortical impact injury affects dopaminergic transmission in the rat striatum. *J Neurochem* 2005; **95**: 457–465.
- Wagner AK, Drewencki L, Chen X, Santos FR, Khan AS, Harun R *et al*. Chronic methylphenidate treatment enhances striatal dopamine neurotransmission after experimental traumatic brain injury. *J Neurochem* 2009; **108**: 986–997.
- Warden DL, Gordon B, McAllister TW, Silver JM, Barth JT, Bruns J *et al*. Guidelines for the pharmacologic treatment of neurobehavioral sequelae of traumatic brain injury. *J Neurotrauma* 2006; **23**: 1468–1501.
- Gu Z, Feng X, Dong X, Chan P. Smoking, genes encoding dopamine pathway and risk for Parkinson's disease. *Neurosci Lett* 2010; **482**: 31–34.
- Xu X, Mill J, Sun B, Chen CK, Huang YS, Wu YY *et al*. Association study of promoter polymorphisms at the dopamine transporter gene in attention deficit hyperactivity disorder. *BMC Psychiatry* 2009; **9**: 3.
- Comings DE, Comings BG, Muhleman D, Dietz G, Shahbahrani B, Tast D *et al*. The dopamine D2 receptor locus as a modifying gene in neuropsychiatric disorders. *J Am Med Assoc* 1991; **266**: 1793–1800.
- Genro JP, Polanczyk GV, Zeni C, Oliveira AS, Roman T, Rohde LA *et al*. A common haplotype at the dopamine transporter gene 5' region is associated with attention-deficit/hyperactivity disorder. *Am J Med Genet B Neuropsychiatr Genet* 2008; **147B**: 1568–1575.
- Drevets WC, Gautier C, Price JC, Kupfer DJ, Kinahan PE, Grace AA *et al*. Amphetamine-induced dopamine release in human ventral striatum correlates with euphoria. *Biol Psychiatry* 2001; **49**: 81–96.
- Laruelle M, Slifstein M, Huang Y. Positron emission tomography: imaging and quantification of neurotransmitter availability. *Methods* 2002; **27**: 87–299.
- Forsback S, Marjamaki P, Eskola O, Bergman J, Rokka J, Gronroos T *et al*. [18F]CFT synthesis and binding to monoamine transporters in rats. *EJNMMI Res* 2012; **2**: 3.
- Zhen J, Ali S, Dutta AK, Reith ME. Characterization of [^3H]CFT binding to the norepinephrine transporter suggests that binding of CFT and nisoxetine is not mutually exclusive. *J Neurosci Methods* 2012; **203**: 19–27.
- Hoffman AF, Lupica CR, Gerhardt GA. Dopamine transporter activity in the substantia nigra and striatum assessed by high-speed chronoamperometric recordings in brain slices. *J Pharmacol Exp Ther* 1998; **287**: 487–496.
- Gurevich EV, Joyce JN. Distribution of dopamine D3 receptor expressing neurons in the human forebrain: comparison with D2 receptor expressing neurons. *Neuropsychopharmacology* 1999; **20**: 60–80.
- Seeman P, Wilson A, Gmeiner P, Kapur S. Dopamine D2 and D3 receptors in human putamen, caudate nucleus, and globus pallidus. *Synapse* 2006; **60**: 205–211.
- Nagren K, Muller L, Halldin C, Swahn CG, Lehtikoinen P. Improved synthesis of some commonly used PET radioligands by the use of [^{11}C]methyl triflate. *Nucl Med Biol* 1995; **22**: 235–239.
- Halldin C, Farde L, Hogberg T, Hall H, Strom P, Ohlberger A *et al*. A comparative PET-study of five carbon-11 or fluorine-18 labelled salicylamides. Preparation and in vitro dopamine D-2 receptor binding. *Int J Rad Appl Instrum B* 1991; **18**: 871–881.
- Wong DF, Yung B, Dannals RF, Shaya EK, Ravert HT, Chen CA *et al*. In vivo imaging of baboon and human dopamine transporters by positron emission tomography using [^{11}C]WIN 35,428. *Synapse* 1993; **15**: 130–142.
- Meltzer CC, Kinahan PE, Greer PJ, Nichols TE, Comtat C, Cantwell MN *et al*. Comparative evaluation of MR-based partial-volume correction schemes for PET. *J Nucl Med* 1999; **40**: 2053–2065.
- Logan J. A review of graphical methods for tracer studies and strategies to reduce bias. *Nucl Med Biol* 2003; **30**: 833–844.
- Wu Y, Carson RE. Noise reduction in the simplified reference tissue model for neuroreceptor functional imaging. *J Cereb Blood Flow Metab* 2002; **12**: 1440–1452.
- Innis RB, Cunningham VJ, Delforge J, Fujita M, Gunn RN, Holden J *et al*. Consensus nomenclature for in vivo imaging of reversibly binding radioligands. *J Cereb Blood Flow Metab* 2007; **27**: 1533–1539.
- Gunn RN, Lammertsma AA, Hume SP, Cunningham VJ. Parametric imaging of ligand-receptor binding in PET using a simplified reference region model. *Neuroimage* 1997; **6**: 279–287.
- Volkow ND, Gur RC, Wang GJ, Fowler JS, Moberg PJ, Ding YS *et al*. Association between decline in brain dopamine activity with age and cognitive and motor impairment in healthy individuals. *Am J Psychiatry* 1998; **155**: 344–349.
- Heinz A, Goldman D, Jones DW, Palmour R, Hommer D, Gorey JG *et al*. Genotype influences in vivo dopamine transporter availability in human striatum. *Neuropsychopharmacology* 2000; **22**: 133–139.
- van Dyck CH, Malison RT, Jacobsen LK, Seibyl JP, Staley JK, Laruelle M *et al*. Increased dopamine transporter availability associated with the 9-repeat allele of the SLC6A3 gene. *J Nucl Med* 2005; **46**: 745–751.
- Ouchi Y, Yoshikawa E, Okada H, Futatsubashi M, Sekine Y, Iyo M *et al*. Alterations in binding site density of dopamine transporter in the striatum, orbitofrontal cortex, and amygdala in early parkinson's disease: compartment analysis for β -CFT binding with positron emission tomography. *Ann Neurol* 1999; **45**: 601–610.
- Rinne JO, Portin R, Ruottinen H, Nurmi E, Bergman J, Haaparanta M *et al*. Cognitive impairment and the brain dopaminergic system in Parkinson disease: [^{18}F]fluorodopa positron emission tomographic study. *Arch Neurol* 2000; **57**: 470–475.
- Lin Z, Canales JJ, Björqvinnson T, Thomsen M, Qu H, Liu QR *et al*. Monoamine transporters: vulnerable and vital doorkeepers. *Prog Mol Biol Transl Sci* 2011; **98**: 1–46.
- McDougall SA, Der-Ghazarian T, Britt CE, Varela FA, Crawford CA. Postnatal manganese exposure alters the expression of D2L and D2S receptor isoforms: relationship to PKA activity and Akt levels. *Synapse* 2011; **65**: 583–591.

- 34 Rumpel R, Alam M, Klein A, Ozer M, Wesemann M, Jin X *et al*. Neuronal firing activity and gene expression changes in the subthalamic nucleus after transplantation of dopamine neurons in hemiparkinsonian rats. *Neurobiol Dis* 2013; **59**: 230–243.
- 35 Volkow ND, Fowler JS, Wang GJ, Hitzemann R, Logan J, Schlyer DJ *et al*. Decreased dopamine D2 receptor availability is associated with reduced frontal metabolism in cocaine abusers. *Synapse* 1993; **14**: 169–177.
- 36 Ritchie T, Noble EP. Association of seven polymorphisms of the D2 dopamine receptor gene with brain receptor-binding characteristics. *Neurochem Res* 2003; **28**: 73–82.
- 37 Noble EP, Gottschalk LA, Fallon JH, Ritchie TL, Wu JC. D2 dopamine receptor polymorphism and brain regional glucose metabolism. *Am J Med Genet* 1997; **74**: 162–166.
- 38 Frank MJ, Hutchison K. Genetic contributions to avoidance-based decisions: striatal D2 receptor polymorphisms. *Neuroscience* 2009; **164**: 131–140.
- 39 Bertolino A, Taurisano P, Pisciotta NM, Blasi G, Fazio L, Romano R *et al*. Genetically determined measures of striatal D2 signaling predict prefrontal activity during working memory performance. *PLoS One* 2010; **5**: e9348.
- 40 Duan J, Wainwright MS, Comeron JM, Saitou N, Sanders AR, Gelernter J *et al*. Synonymous mutations in the human dopamine receptor D2 (DRD2) affect mRNA stability and synthesis of the receptor. *Hum Mol Genet* 2003; **12**: 205–216.
- 41 Troiano AR, Schulzer M, de la Fuente-Fernandez R, Mak E, McKenzie J, Sossi V *et al*. Dopamine transporter PET in normal aging: dopamine transporter decline and its possible role in preservation of motor function. *Synapse* 2010; **64**: 146–151.
- 42 Bruck A, Portin R, Lindell A, Laihinien A, Bergman J, Haaparanta M *et al*. Positron emission tomography shows that impaired frontal lobe functioning in parkinson's disease is related to dopaminergic hypofunction in the caudate nucleus. *Neurosci Lett* 2001; **311**: 81–84.
- 43 Rohde LA, Roman T, Szobot C, Cunha RD, Hutz MH, Biederman J. Dopamine transporter gene, response to methylphenidate and cerebral blood flow in attention-deficit/hyperactivity disorder: a pilot study. *Synapse* 2003; **48**: 87–89.
- 44 Zhang ZY, Zhang Z, Fauser U, Schluesener HJ. Global hypomethylation defines a sub-population of reactive microglia/macrophages in experimental traumatic brain injury. *Neurosci Lett* 2007; **429**: 1–6.
- 45 Abdolmaleky HM, Smith CL, Zhou JR, Thiagalingam S. Epigenetic alterations of the dopaminergic system in major psychiatric disorders. *Methods Mol Biol* 2008; **448**: 187–212.